A Novel Cladding Structure for Semiconductor Quantum-Well Lasers with Small Beam Divergence and Low Threshold Current

Shun-Tung Yen and Chien-Ping Lee, *Senior Member, IEEE*

Abstract— **A novel cladding structure is proposed and analyzed for semiconductor quantum-well lasers to achieve a small vertical-beam divergence and a low threshold current density simultaneously. This cladding structure is designed to guide a wide optical mode but with a high peak intensity in quantum wells. The wide expansion of the optical mode results in a small beam divergence. In addition, the high optical intensity in quantum wells causes a low threshold current density. This novel cladding structure is optimized. The result shows that this type of cladding structures can achieve a beam divergence as small as 14.6° while the threshold current density remains small.**

I. Introduction

SEMICONDUCTOR lasers with small beam divergence are desired for efficient coupling of laser output into another device. Especially for lasers used to pump fiber amplifiers, high pumping power is needed to achieve high gain. To obtain high pumping power, the pump lasers are required with a small beam divergence as well as a high output power. However, in semiconductor quantum-well (QW) lasers with conventional uniform cladding layers, a small beam divergence is generally accompanied by an unacceptable high threshold current. Undesired low conversion efficiency then results and degrades the performance in high-power operation.

To cure this problem, several semiconductor lasers with unconventional cladding structures have been proposed and studied [1]–[8]. Wu *et al.* utilized periodic-index optical confining layers in 980-nm semiconductor lasers to achieve high-power coupling into a single-mode fiber [1], [2]. Cockerill *et al.* obtained a reduced beam divergence with acceptable low threshold current density by using a depressed index cladding graded barrier structure [3], [4]. Chen *et al.* integrated passive waveguides in the cladding layers and obtained a beam divergence of 11.2° but with serious side lobes [5], [6]. Recently, the authors theoretically studied in detail the performance of the QW lasers with passive waveguides integrated in the cladding layers [7]. The results show that a small beam divergence without side lobes can be achieved at a price of only a slight increase in threshold current density. Using the structure, Ziari *et al.* achieved low-loss coupling of only −1 dB into a single-mode fiber [8].

Manuscript received October 18, 1995; revised May 6, 1996. This work was supported in part by the National Science Council of the Republic of China under Contract NSC84-2215-E009-039.

The authors are with the Department of Electronics Engineering, National Chiao Tung University, Hsinchu, Taiwan, Republic of China.

Publisher Item Identifier S 0018-9197(96)06284-7.

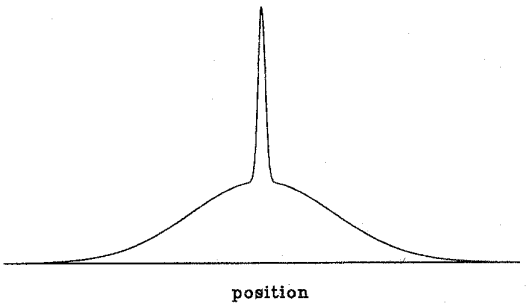

Fig. 1. The desired lasing-mode profile for low threshold current and small beam divergence.

These studies have revealed an important concept that the intensity profile of an optical mode can be engineered by manipulating the spatial variation of the refractive index of cladding layers. The desired optical mode profile for both low threshold current and small beam divergence is shown in Fig. 1. This profile is widely expanded but has a high intensity in the center (in the active region). For semiconductor QW lasers, a low threshold current density can be obtained due to the high optical intensity in the quantum wells. Meanwhile, a small beam divergence can be achieved since the optical mode is widely expanded.

In this paper, we propose and analyze a novel type of cladding structure for semiconductor QW lasers to guide the desired optical mode shown in Fig. 1. The novel cladding structure is reached in the following way. We first start with a wave function that gives small beam divergence and low threshold. From the wave function, we then construct the laser structure that supports such a mode. Once the laser structure is obtained, detailed analysis is performed by exact calculation. The dependence of the threshold current density and the output beam divergence on the structure parameters is interpreted in detail. Based on the calculated results, the cladding structure is then optimized. The optimized structure can have a vertical far-field angle as small as 14.6° while maintaining a low threshold current density (180 A/cm^2) for a 1-mm-long single QW InGaAs–AlGaAs laser. This paper is organized as follows. In the following section, we first search for the cladding structure that guides the desired optical mode. The resulting cladding structure is then analyzed and optimized by using exact calculation in Section III. In Section IV, the sensitivity of laser performance to structural

parameters is discussed. Finally, we draw a conclusion in Section V.

II. Search for Desired Cladding Structures

To give a comprehensible concept of the characteristic of the novel structure, we first describe the optical mode guided by the structure in an illustrative way. The desired optical mode shown in Fig. 1 for QW lasers can be expressed in a linear combination of two functions $\psi_{\rm tc}(x)$ and $\psi_{\rm we}(x)$ as

$$\psi(x) = A_{\rm tc}\psi_{\rm tc}(x) + A_{\rm we}\psi_{\rm we}(x) \tag{1}$$

where $\psi_{\rm tc}(x)$ is a wave function tightly confined in the core region and $\psi_{\rm we}(x)$ is a widely expanded wave function. $\psi_{\rm tc}(x)$ and $\psi_{\rm we}(x)$ are assumed to be normalized. $A_{\rm tc}$ and $A_{\rm we}$ are chosen so that $\psi(x)$ is also normalized. If $|\psi_{\rm tc}(x)|^2 \gg |\psi_{\rm we}(x)|^2$ in the quantum well, for example, $|\psi_{\rm tc}(x)|^2 \approx \delta(x)$, it is possible to choose an $A_{\rm tc}$ so that $A_{\rm tc} \ll A_{\rm we}$ but $|A_{\rm tc}\psi_{\rm tc}(x)|^2$ is still much lager than $|A_{\rm we}\psi_{\rm we}(x)|^2$ in the quantum well. By $A_{\rm tc} \ll A_{\rm we}$, it means that most of the optical power of the mode is from the second term in (1), $A_{\rm we}\psi_{\rm we}(x)$, which, due to its wide expansion, causes a small beam divergence. The threshold current density is determined only by the optical intensity in the quantum well. Because $|A_{\rm tc}\psi_{\rm tc}(x)|^2$ is much lager than $|A_{\rm we}\psi_{\rm we}(x)|^2$ in the quantum well, the threshold current density can remain low and is not much affected by the wide expansion of the optical mode.

The above illustration indicates that both a very small beam divergence and a very low threshold current density can be obtained simultaneously if $\psi_{\rm tc}(x)$ has a very high intensity in the quantum well. In reality, however, the spatial variation of the optical-mode profile is governed by the spatially varying refractive index throughout the laser structure. Due to the limitation of the available materials for semiconductor lasers, one can not obtain an optical mode with an arbitrary profile. The condition which restricts the optical-mode profile is that the spatially varying refractive index

$$n(x) = \sqrt{n_{\rm eff}^2 - \frac{\psi(x)}{k_0^2\psi(x)}} \tag{2}$$

is within the limit of the available materials. Here, (2) is obtained from the one-dimensional wave equation. $n_{\rm eff}$ is the effective refractive index or the mode index and k_0 is the wave number in free space. In spite of this inherent limitation, one can tailor the cladding structure to obtain an optical mode as close to that shown in Fig. 1 as possible.

It is interesting to see what kind of cladding structures can result in the desired optical mode shown in Fig. 1. To do this, we first choose the tightly confined wave function $\psi_{\rm tc}(x)$ and the widely expanded wave function $\psi_{\rm we}(x)$. After the wave functions are determined, the cladding structure can be found by using the relation (2). Assume that the tightly confined wave $\psi_{\rm tc}(x)$ is guided by the waveguide structure shown in Fig. 2, which is a linearly graded separate-confinement heterostructure (GRINSCH) generally used in QW lasers. The structure is composed of a 65-Å $In_{0.2}Ga_{0.8}As$ quantum well, two 150-Å GaAs confining layers, two linearly graded layers, and two uniform $Al_xGa_{1-x}As$ cladding layers. We choose $\psi_{\rm tc}(x)$ with a large confinement factor by optimizing the thickness of the linearly graded layers and the Al content x in the cladding layers. Fig. 3 shows the plots of the confinement factor, the threshold current density, the full width at half maximum (FWHM) of the far-field pattern versus the thickness of the graded layer for the lasing mode of the GRINSCH shown in Fig. 2. Three different Al contents, $x = 0.4$, 0.6, and 0.8, of cladding layers are considered. Here, the optical modes are obtained by solving the one-dimensional wave equation using the Galerkin method [9]. Since the structure is assumed to be symmetric and only the optical modes with the even parity are considered (because the optical modes with the odd parity never oscillate), the trigonometric cosine functions are employed as basis functions to expand the optical modes. The number of the basis functions is chosen to be one hundred so that the precision in the calculated results is assured. We have checked the accuracy of this method by comparing some of the results with those obtained by the conventional transfer-matrix method. Basically, no difference is observed. The advantage of the Galerkin method is that all the eigenmodes can be obtained simultaneously by diagonalizing a matrix, which significantly reduces the computation time. Once the optical modes have been calculated, the lasing mode which has the highest confinement factor of all the modes is selected. The far-field pattern of the lasing mode is then calculated using the expression [10], [11]

$$\frac{|\phi(\Theta)|^2}{|\phi(0)|^2} = \frac{|g(\Theta)|^2}{|g(0)|^2}\frac{\left|\int_{-\infty}^{\infty}\psi(x)\exp(ik_0x\sin\Theta)dx\right|^2}{\left|\int_{-\infty}^{\infty}\psi(x)dx\right|^2} \tag{3}$$

where $\psi(x)$ is the near field and $\phi(\Theta)$ is the far field at angle Θ. The Huygen's correction factor $g(\Theta)$ is chosen as [10]

$$g(\Theta) = \frac{\cos\Theta}{\cos\Theta + n_{\rm eff}}. \tag{4}$$

In calculating the threshold current density, we assume the laser is 1 mm long and use the empirical formula

$$J_{\rm th} = \frac{J_0}{\eta_i}\exp\left(\frac{\alpha_t}{\Gamma b_0 J_0}\right) \tag{5}$$

where $J_0 = 50$ A/cm^2 is the transparency current density, $\eta_i = 0.97$ is the internal quantum efficiency, $b_0 = 24$ cm/A is the gain coefficient, and $\alpha_t = 20$ cm^{-1} is the total loss for a 1-mm-long cavity. These parameters have been determined experimentally for the GRINSCH laser shown in Fig. 2 [12]. From Fig. 3(a), one can find that too thin or too thick graded layers are not preferable for a high confinement factor. The confinement factor reaches the maximum when the graded layer thickness is 1000 Å and the Al content in cladding layers is 0.8. We choose these structure parameters for the waveguide shown in Fig. 2 and calculate the lasing mode to obtain the tightly confined wave function $\psi_{\rm tc}(x)$. Note that for this structure, although the threshold current density reaches the minimum, the FWHM of the far-field pattern is 60°, which is unacceptable for the actual application in optical coupling to fibers.

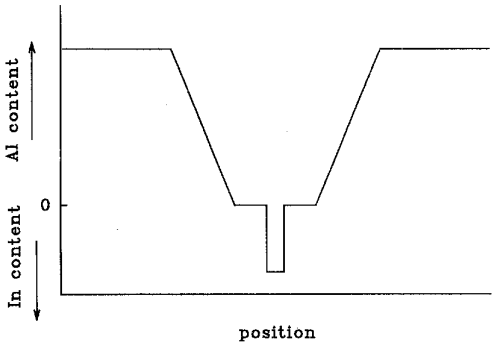

Fig. 2. The waveguide structure (the conventional GRINSCH) guiding the tightly confined wave $\psi_{\rm tc}(x)$. The structure is composed of a 65-Å $In_{0.2}Ga_{0.8}As$ quantum well, two 150-Å GaAs confining layers, two linearly graded layers, and two uniform $Al_xGa_{1-x}As$ cladding layers.

The widely expanded wave function $\psi_{\rm we}(x)$ is, for illustration purposes, assumed to be

$$\psi_{\rm we}(x) = \sqrt{\frac{2}{L}}\cos\left(\frac{\pi x}{L}\right) \quad \text{for } -\frac{L}{2} < x < \frac{L}{2} \qquad (6)$$
$$= 0 \quad \text{elsewhere}$$

for L large enough.[1]

Once $\psi_{\rm tc}(x)$ and $\psi_{\rm we}(x)$ have been determined, one can investigate the laser performance resulting from the combined wave function $\psi(x) = A_{\rm tc}\psi_{\rm tc}(x) + A_{\rm we}\psi_{\rm we}(x)$ by varying the coefficient $A_{\rm tc}$ and the width L of the optical mode [see (6)]. Fig. 4 shows the plots for the combined wave function $\psi(x)$, the confinement factor, the threshold current density, FWHM of the far-field pattern, and the standard deviation of far field angle, σ_Θ (the rms of far-field angle), versus the coefficient $A_{\rm tc}$ with the width L as a parameter (L = 2, 4, 6, and 8 μm). The standard deviation of far field angle, σ_Θ, is defined as

$$\sigma_\Theta = \left[\frac{\int_{-\frac{\pi}{2}}^{\frac{\pi}{2}} |\phi(\Theta)|^2\Theta^2 d\Theta}{\int_{-\frac{\pi}{2}}^{\frac{\pi}{2}} |\phi(\Theta)|^2 d\Theta}\right]^{\frac{1}{2}}. \qquad (7)$$

Here, σ_Θ is considered because FWHM is not a good measure of the beam divergence when serious side lobes appear. As expected, in Fig. 4(a), the confinement factor increases with the amplitude $A_{\rm tc}$ of the tightly confined wave and decreases with the width L of the widely expanded wave. The resulting threshold current density shown in Fig. 4(b) therefore decreases with $A_{\rm tc}$ and increases with the width L. The threshold current density, however, changes slowly when $A_{\rm tc} > 0.5$ because the argument of the exponential function in formula (5) remains small for $A_{\rm tc} > 0.5$. This small argument of the exponential function is generally true for long cavity 980-nm InGaAs–AlGaAs lasers. From Fig. 4(c) and (d), one can find that FWHM and σ_Θ decrease with the decrease of $A_{\rm tc}$ more rapidly than the threshold current density increases with the decrease of $A_{\rm tc}$. This makes it possible, by a properly chosen $A_{\rm tc}$ ($\approx$0.5), to significantly improve the beam divergence by paying only a very small price in the threshold current density. We also notice that for large L's, around $A_{\rm tc} \approx 1$, FWHM decreases much more drastically with the decrease of $A_{\rm tc}$ than σ_Θ does. Here, a small FWHM does not mean a good beam divergence because σ_Θ is still large. This implies that the far-field pattern has serious side lobes. For a smaller L, i.e., for a narrower $\psi_{\rm we}(x)$, the beam divergence is not improved as

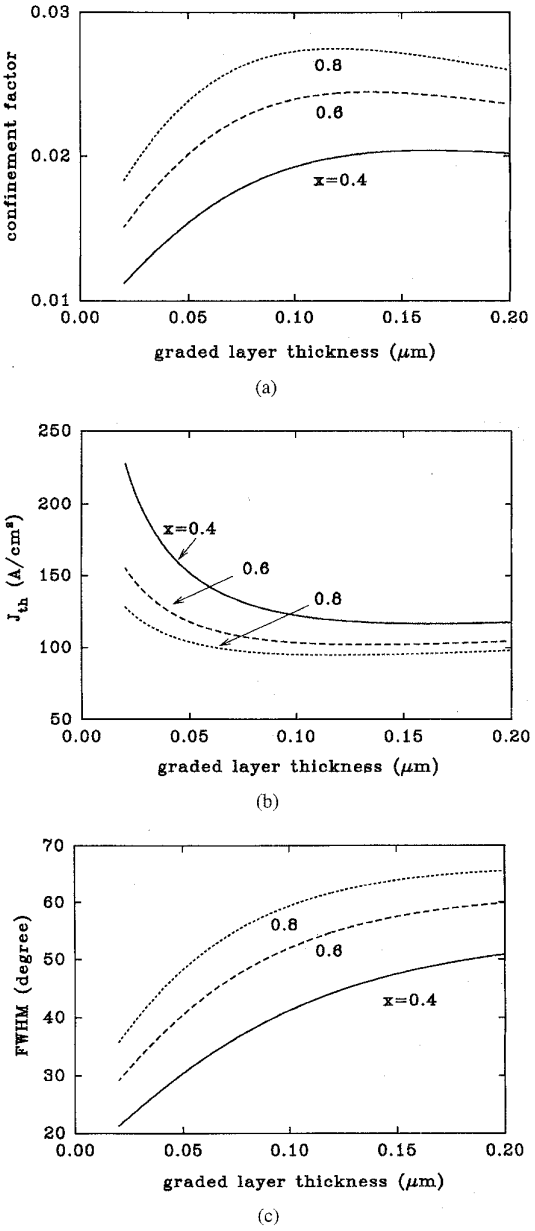

Fig. 3. (a) The confinement factor, (b) the threshold current density, and (c) FWHM of the far-field pattern versus the thickness of the graded layers for the conventional GRINSCH laser. Three different Al contents of cladding layers, x = 0.4, 0.6, and 0.8 are considered.

[1]The assumption of the wave function $\psi_{\rm we}(x)$ in (6) implies that the waveguide structure guiding $\psi_{\rm we}(x)$ has an infinite change in the refractive index at $x = \pm L/2$. It is impossible in practice to have an infinite change in the refractive index. However, when L is large enough, even for a slight change in the refractive index at $x = \pm L/2$ most of the optical field of the widely expanded mode $\psi_{\rm we}(x)$ is distributed within the region $-L/2 < x < L/2$ and a negligible amount of optical field penetrates out of this region. In this situation, the cosine function in (6) is a good approximation for the real optical mode.

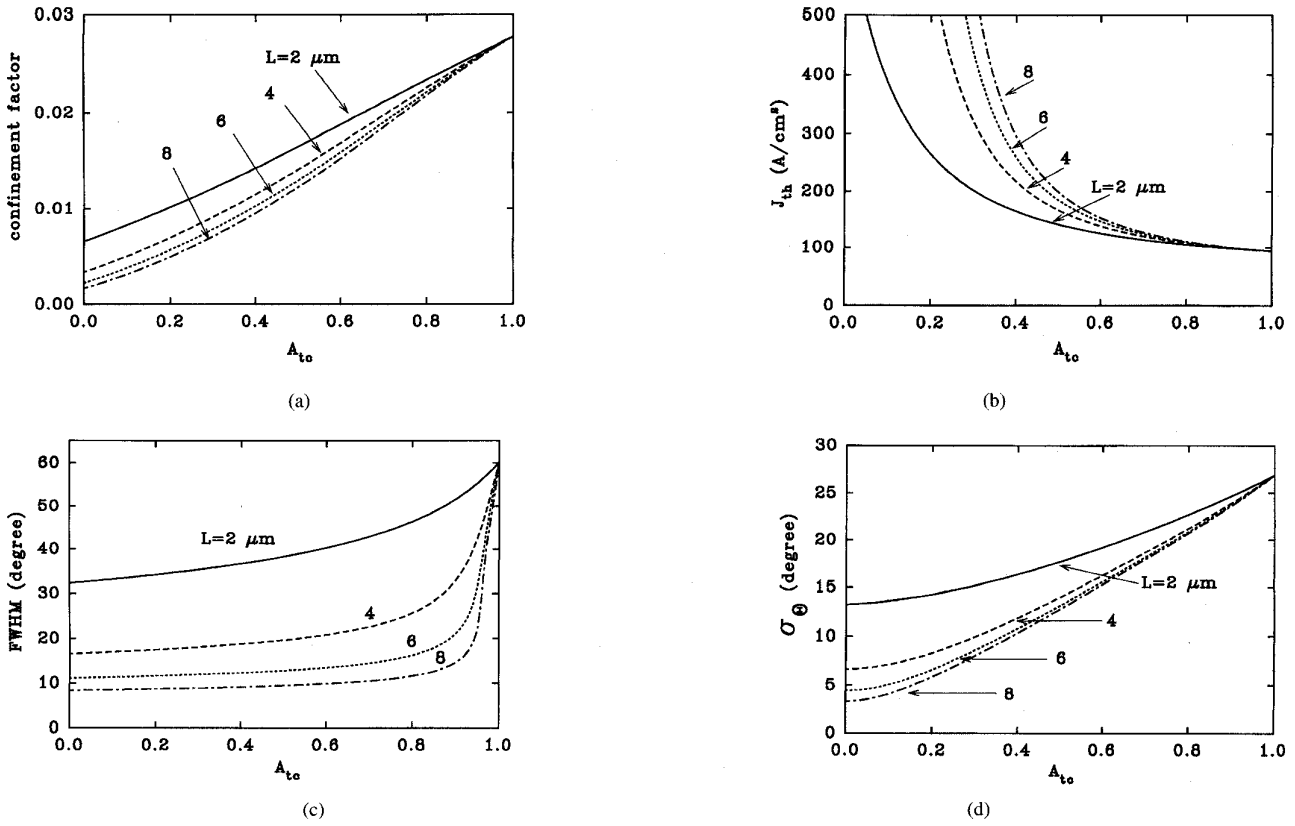

Fig. 4. (a) The confinement factor, (b) the threshold current density, (c) FWHM of the far-field pattern, and (d) σ_Θ versus $A_{\rm tc}$ for the combined optical mode $\psi(x) = A_{\rm tc}\psi_{\rm tc}(x) + A_{\rm we}\psi_{\rm we}(x)$. Four L's, L = 2, 4, 6, and 8 μm, are considered.

much as for large L's because the optical mode is not widely expanded.

Shown in Fig. 5(a) and (b) are the near-field and the far-field intensities, respectively, for the tightly confined wave $\psi_{\rm tc}(x)$, the widely expanded wave $\psi_{\rm we}(x)$, and the combined wave $\psi(x) = A_{\rm tc}\psi_{\rm tc}(x) + A_{\rm we}\psi_{\rm we}(x)$ with $A_{\rm tc} = 0.5$. The width L for $\psi_{\rm we}(x)$ is chosen to be 6 μm. One can see from Fig. 4 that if $A_{\rm tc} = 0.5$ and $L = 6$ μm, low threshold current and small beam divergence can be obtained simultaneously. Although the confinement factor of $\psi(x)$ is significantly different from that of $\psi_{\rm tc}(x)$, the threshold current density of $\psi(x)(\approx 180$ A/cm^2) is less than twice of that of $\psi_{\rm tc}(x)(\approx 100$ A/cm^2). However, FWHM and σ_Θ are improved from 60° and 37° for $\psi_{\rm tc}(x)$ to 12.8° and 13.1° for $\psi(x)$, respectively.

Now that the desired combined optical mode $\psi(x)$ is determined [e.g., the solid curve in Fig. 5(a)], the spatially varying refractive index which guides the combined wave $\psi(x)$ can be obtained by using the relation (2). Neglecting the existence of the $In_{0.2}Ga_{0.8}As$ quantum well and assuming the refractive index at $x = 0$, $n(0)$, is that of GaAs, we obtain the spatially varying refractive index $n(x)$ shown in Fig. 6. The dotted line in the figure represents the effective refractive index $n_{\rm eff}$ of the combined mode. From the figure, we find some interesting features. First, there are two low refractive-index layers around the active region. The two low-index layers similar to the depressed layers used in [3] tend to tightly confine the optical field in the active region. Additionally, the effective refractive index $n_{\rm eff}$ of the optical mode is lowered by these two layers. As $n_{\rm eff}$ moves toward the refractive index of the flat cladding region, the optical intensity decays slowly outside of the two low-index layers and the optical mode is widely expanded. If the effective refractive index $n_{\rm eff}$ is much higher than the refractive index of the flat cladding region, the optical field will decay rapidly in the cladding, resulting in an undesirable narrow optical mode. However, if the effective refractive index $n_{\rm eff}$ is lower than the refractive index of the flat cladding region, the danger of higher order mode oscillation may result. This is because the mode with the highest confinement factor may come from a higher order mode. Similar behavior has been observed for QW lasers with passive waveguides [7] and explained using the coupled-mode theory. In this situation, the far-field pattern of the laser becomes very poor. To avoid this danger of higher order mode oscillation but still maintain a widespread mode, one has to control the lasing mode with the mode index safely higher but close to the refractive index of the flat cladding region.

It is worth mentioning that in our calculated results (Fig. 6), the effective refractive index of the fundamental mode (indicated as the dotted line) is slightly lower than the refractive index of the flat cladding region. This results from the assumption of the cosine function in (6) for $\psi_{\rm we}(x)$. If one assumes that the $\psi_{\rm we}(x)$ has exponentially decaying tails, as in real situations, one will obtain the lasing mode index $n_{\rm eff}$ higher

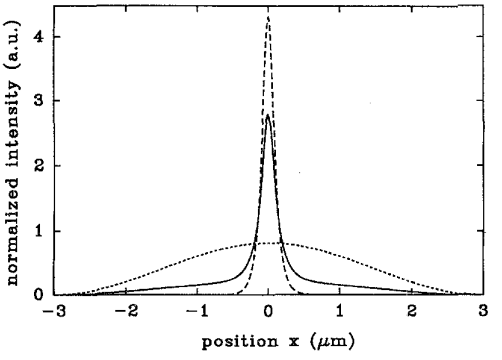

(a)

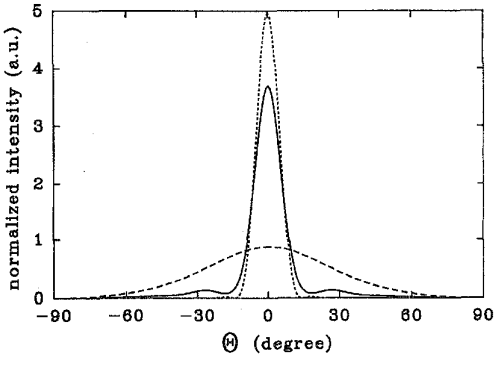

(b)

Fig. 5. (a) The near-field and (b) the far-field intensities for the combined wave $\psi(x)$ with $A_{tc} = 0.5$ (the solid line), the tightly confined wave $\psi_{tc}(x)$ (the dashed line), and the widely expanded wave $\psi_{we}(x)$ (the dotted line) with the width L of 6 μm.

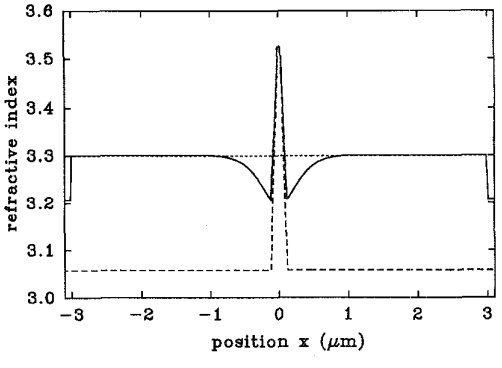

Fig. 6. The spatially varying refractive index of the structure guiding the combined wave $\psi(x)$ with $A_{tc} = 0.5$ and $L = 6$ μm (the solid line) and that guiding the tightly confined wave $\psi_{tc}(x)$ (the dashed line). The dotted line is shown for the effective refractive index of the optical mode.

than the refractive index of the flat cladding region, and there will not be any mode instability.

III. Analysis and Optimization of Cladding Structure

Based on the description presented in the previous section, we can now propose the structure shown in Fig. 7 for low threshold current and small beam divergence. The structure is similar to the one shown in Fig. 6, except that in Fig. 7 the outer graded layers (with thickness C) are assumed to

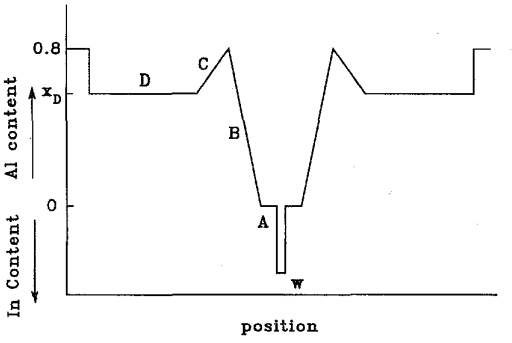

Fig. 7. The proposed structure for low threshold current and small beam divergence. The structure is composed of a 65-Å $In_{0.2}Ga_{0.8}As$ quantum well, two 150-Å GaAs confining layers, two 1000-Å inner linearly graded layers with Al content from 0 to 0.8, two outer linearly graded layers with thickness of C and Al content from 0.8 to x_D, and two cladding layers with thickness of D and Al content x_D. Out of these layers are two high-Al-content ($x = 0.8$) layers for confining the optical field.

be graded linearly. In this structure, the quantum well, the confining layers, and the inner linearly graded layers are assumed to be the same as those shown in Fig. 2 with 80% Al content in the cladding layers. The Al content in the outer graded layer is linearly changed from $x = 0.8$ to $x = x_D$, where then the Al content is kept constant for a length D before it is increased to $x = 0.8$ in the outermost layers. The layers with Al content of x_D and thickness of D are called, for convenience, the flat cladding layers. The high-Al-content ($x = 0.8$) layers outside the flat cladding layers are used to force the optical intensity to attenuate rapidly. In the following, we will analyze the performance of this type of laser by varying the outer graded layer thickness C, the flat cladding layer thickness D, and the Al content x_D of the flat cladding layers. The laser cavity length is assumed to be 1 mm. As before, the optical modes of the entire structure are calculated exactly using the Galerkin method with one hundred cosine functions as the basis. The far-field pattern and the threshold current density are calculated using (3) and (5), respectively.

In Fig. 8, we show the plots of the threshold current density, FWHM of the far-field pattern, and σ_Θ versus the Al content, x_D, of the flat cladding layers for different flat cladding layer thicknesses, $D = 1$, 2, 3, and 4 μm. The outer graded layer thickness C is 0.2 μm. From Fig. 8(a), we see that the threshold current density remains very low when x_D is larger than 0.45 for all the four flat cladding layer thicknesses. This means that the two low-index layers maintain high optical intensity in the active region for $x_D > 0.45$. However, the FWHM shown in Fig. 8(b) is improved significantly from 60° (for $x_D = 0.8$) to $\approx 10°$ (for $x_D \approx 0.45$) for thick flat cladding layers, such as $D = 3$ or 4 μm. This means that the optical field leaks out of the active region with the decrease of x_D. The far-field pattern is more sensitive to the expansion of the optical mode than is the threshold current density. As a result, one can choose $D = 3$ or 4 μm and $x_D \approx 0.45$ to simultaneously achieve a very low threshold current density and a very good beam divergence. The improvement on the beam divergence for $D = 1$ μm is not so much as that for $D = 3$ or 4 μm. This is because for $D = 1$ μm, the optical field is more tightly

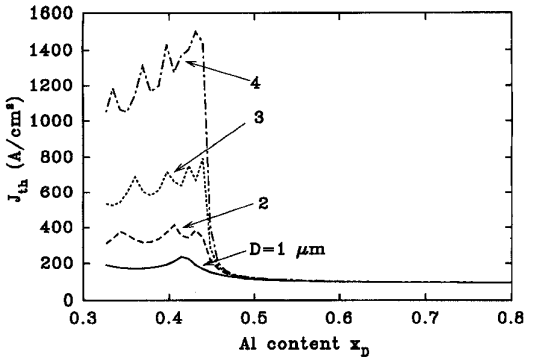

(a)

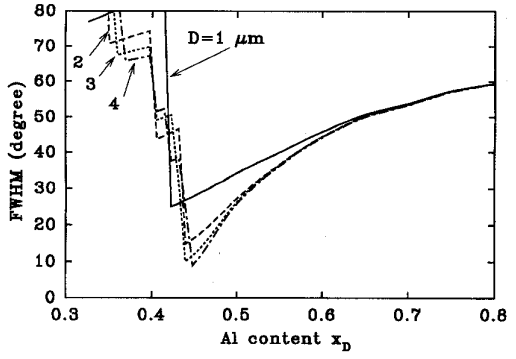

(b)

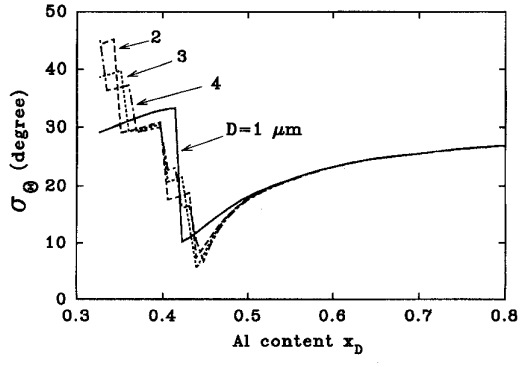

(c)

Fig. 8. (a) The threshold current density, (b) FWHM, and (c) σ_Θ versus the Al content in the cladding layers x_D for different cladding layer thicknesses, D = 1, 2, 3, and 4 μm. The outer graded layer thickness C is 0.2 μm.

confined than for larger D's. It can be also seen from these figures that the performances for $D = 3$ μm differ very little from those for $D = 4$ μm when $x_D > 0.45$. The reason is that for very thick flat cladding layers with $x_D > 0.45$, the optical intensity attenuates to nearly zero at the interfaces between the thick flat cladding layers and the two outermost layers. Therefore, the outermost layers become useless. For practical considerations, 3-μm cladding layers are preferred to the 4-μm or thicker flat cladding layers because of easier material growth and better electrical and thermal properties.

Note that there is an abrupt change in the beam divergence around $x_D \approx 0.45$. This is because when $x_D < 0.45$, the lasing mode index n_{eff} falls lower than the refractive index of the flat cladding layers. As described in the previous section, once this situation occurs, the lasing mode switches from the fundamental mode to a higher order mode. The far-field pattern thus becomes very poor [see Fig. 8(b) and (c)]. In addition, because the optical modes are no longer bound by the flat cladding layers, the confinement factor of the lasing mode becomes very small. Therefore, the threshold current density in Fig. 8(a) drastically increases for large D's when x_D crosses over the critical value, 0.45. In Fig. 8(b) and (c), the far-field divergence reaches a minimum around $x_D \approx 0.45$. In order to achieve small beam divergence one should control x_D to be within $0.45 \sim 0.5$. In the current material growth technologies, it is not difficult to control the Al content within this region.

Fig. 9 shows the plots of the threshold current density, FWHM, and σ_Θ versus the outer graded layer thickness C for various Al contents of the cladding layers (x_D = 0.45, 0.5, 0.6, and 0.8). Here the flat cladding layer thickness D is chosen to be 3 μm. It can be seen from Fig. 9(a) that for x_D = 0.5, 0.6, and 0.8, the threshold current density is low for all C's. This is because the lasing mode is tightly confined due to a large difference between the lasing mode index and the refractive index of the flat cladding layers. However, for $x_D = 0.45$, the threshold current density changes rapidly with C. This is because the lasing mode index is sensitive to the variation of the thickness C for $x_D \approx 0.45$. As C increases from 0 to ≈ 0.23 μm, the lasing-mode index decreases. Since the lasing-mode index becomes closer to the refractive index of the flat cladding layers, the optical field which leaks out of the active region becomes significant and then the threshold current increase rapidly. As the thickness C further increases and exceeds the critical value 0.23 μm, the lasing-mode index crosses over the refractive index of the flat cladding layers, and the lasing mode switches from the fundamental mode to a higher order mode. This lasing-mode switching causes the abrupt hops in the beam divergence [see the curves for $x_D = 0.45$ in Fig. 9(b) and (c)]. So, for $x_D \approx 0.45$, one should control the thickness C smaller than 0.23 μm for the fundamental operation.

Note that in spite of the low threshold current density for x_D = 0.5, 0.6, and 0.8, the beam divergence is not improved as much as for $x_D = 0.45$. From Fig. 9(c), we see that the improvement on the beam divergence is significant for x_D = 0.45 and $C \approx 0.2$ μm. Fortunately, for this value of C, the threshold current density is still low [see Fig. 9(a)]. It is therefore possible to achieve small beam divergence and low threshold current for a QW laser by choosing $x_D \approx 0.45$ and $C \approx 0.2$ μm.

Fig. 10 shows the normalized near-field intensities and the far-field intensities for two different structures. One is the proposed structure shown in Fig. 7 with $C = 0.2$ μm, $D = 3$ μm, and $x_D = 0.46$. The other is the conventional structure shown in Fig. 2 with 340-Å linear graded layers and 40% Al-content cladding layers. These parameters are chosen intentionally so that the confinement factors for the two structures are the same. From Fig. 10(a), we see that although the optical intensities in the quantum wells of the two structures are the same, the optical mode expands much more widely for the proposed structure than for the conventional one. This wide expansion of

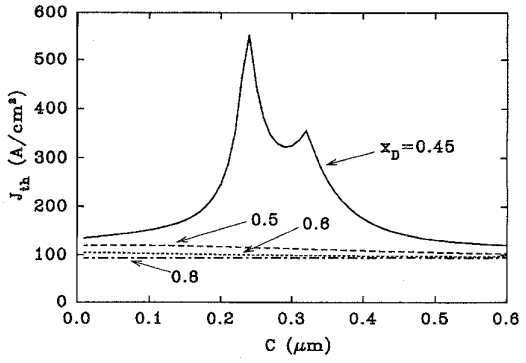

(a)

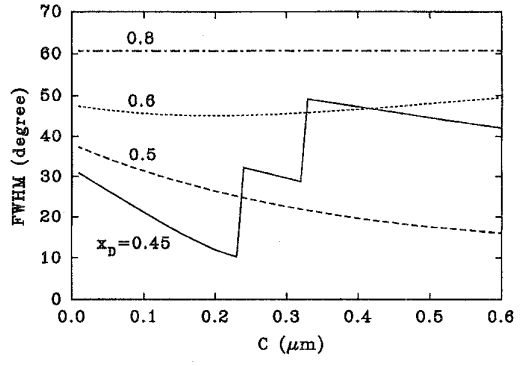

(b)

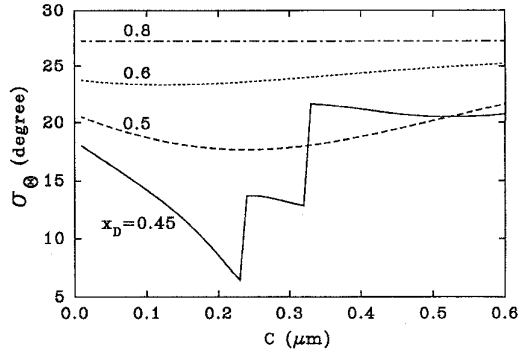

(c)

Fig. 9. (a) The threshold current density, (b) FWHM, and (c) σ_Θ versus the outer graded-layer thickness C for various Al contents in the cladding layers (x_D = 0.45, 0.5, 0.6, and 0.8). The cladding layer thickness D is chosen as 3 μm.

the optical mode causes a significant improvement on the beam divergence [see Fig. 10(b)]. The threshold current densities for the two structures are both 180 A/cm^2 in our calculation. The FWHM and σ_Θ for the conventional structure are 25.8° and 15.6°, respectively, but for the proposed structure, they are as small as 14.6° and 10.7°, respectively. Good far-field patterns with FWHM smaller than 20° are easily achieved while the threshold current density can remain very small by using the proposed cladding structure. This very small beam divergence in the direction perpendicular to the heterointerfaces makes the output beam more symmetric and therefore makes the optical coupling more efficient.

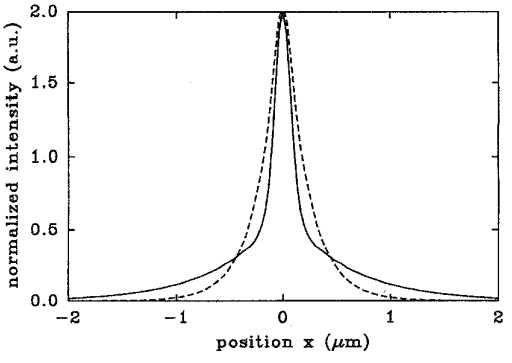

(a)

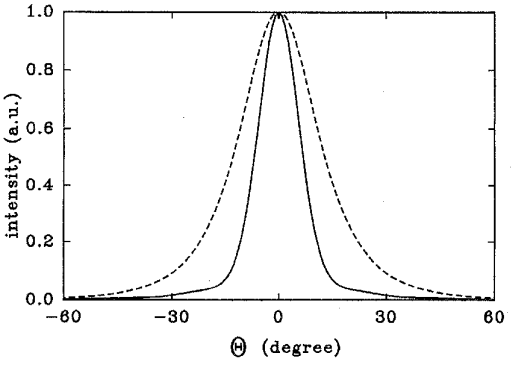

(b)

Fig. 10. (a) The normalized near-field intensities and (b) the far-field intensities for two different structures. One is the proposed structure (shown in Fig. 7) with C = 0.2 μm, D = 3μm, and x_D = 0.46 (the solid line). The other is the conventional structure (shown in Fig. 2) with 340-Å linear graded layers and 0.4 Al-content cladding layers (the dashed line).

IV. Discussion

We have shown theoretically that by properly designing the cladding structure, it is possible to achieve a semiconductor laser with a vertical far-field angle smaller than 15° while maintaining a low threshold current density at the same time. However, to obtain such a narrow beam divergence, one has to precisely control the structure parameters, such as the Al content x_D of the flat cladding layers and the thickness C of the outer graded layers. For the best result, these values need to be close to but not beyond the critical values ($x_D \approx 0.45$ and $C \approx 0.23$ μm). However, when they are close to the critical values, the laser performance becomes very sensitive to the variation of the structural parameters because of the possible higher order mode oscillation. To reduce the sensitivity and maintain a robust design, one should give up pursuing the limit of small beam divergence and sacrifice some of the beam divergence. For example, one can choose $x_D \approx 0.48, C \approx 0.2$ μm, and $D \approx 3$ μm. In this case, the far-field angle is still acceptably small ($\approx 20°$) but without the danger of higher order mode oscillation.

Because of the two low-index (or high-barrier) layers used in our structure, one may question the possibility of the blocking of the injected carriers by the barriers. This is, however, not possible because the low-index layers and the cladding layers, including the flat cladding layers and the outermost layers,

are all heavily doped. Under forward bias, the movement of majority carriers are more or less free in these regions. Very recently, a high-performance InGaAs–AlGaAs QW laser with two low-index layers similar to ours was demonstrated experimentally [13]. A vertical far-field angle of 18° and an optical output power of >500 mW were achieved. This small beam divergence and high output power resulted in a 60% coupling efficiency and >250 mW power coupling to a single-mode fiber. Additionally, the characteristic temperature was improved compared to the conventional structure and the series resistance was as small as $\approx 1.5\ \Omega$. These results indicate that the low-index (or high-barrier) layers will not cause any problem in the laser operation. Although the majority carrier injection is not affected by the low-index layers, the leakage current (caused by the minority carrier flow) is suppressed by the addition of the two wide-bandgap low-index layers. This will improve the characteristic temperature of the new laser structure.

V. Conclusion

We have proposed and analyzed a novel cladding structure for QW semiconductor lasers to simultaneously achieve low threshold current density and small beam divergence. This proposed structure has a tendency to tightly confine the optical field in the active region but tends to loosen the optical field outside of the active region. The threshold current density which is determined by the optical intensity in the quantum well can therefore remain low. Meanwhile, the output beam divergence is improved significantly by the widely expanded field outside of the active region. The structure has been optimized and the result shows that the FWHM can be improved to be as small as 14.6° while the threshold current density remains small (180 A/cm^2) for a 1-mm-long 980-nm InGaAs–AlGaAs laser with the proposed cladding structure. We have also discussed the problem of the sensitivity of laser performance to the structure. By sacrificing some of the beam divergence, one can obtain a stable laser output with a low threshold and still a small beam divergence. It is believed that this type of cladding structure will be very useful for semiconductor lasers.

Acknowledgment

The authors would like to thank the reviewers for their expert and helpful comments.

References

[1] M. C. Wu, Y. K. Chen, M. Hong, J. P. Mannaerts, M. A. Chin, and A. M. Sergent, "A periodic index separate confinement heterostructure quantum well laser," *Appl. Phys. Lett.*, vol. 59, pp. 1046–1048, 1991.

[2] Y. K. Chen, M. C. Wu, W. S. Hobson, M. A. Chin, K. D. Choquette, R. S. Freund, and A. M. Sergent, "High-temperature operation of periodic index separate confinement heterostructure quantum well laser," *Appl. Phys. Lett.*, vol. 59, pp. 2784–2786, 1991.

[3] T. M. Cockerill, J. Honig, T. A. DeTemple, and J. J. Coleman, "Depressed index cladding graded barrier separate confinement single quantum well heterostructure laser," *Appl. Phys. Lett.*, vol. 59, pp. 2694–2696, 1991.

[4] A. C. Crook, C. M. Herzinger, T. M. Cockerill, D. V. Forbes, J. Honig, T. A. DeTemple, J. J. Coleman, I. A. White, and P. A. Besse, "Modal properties of depressed cladding semiconductor waveguides and lasers," *IEEE J. Quantum Electron.*, vol. 30, pp. 2817–2826, 1994.

[5] Y. C. Chen, R. G. Waters, and R. J. Dalby, "Single quantum well laser with vertically integrated passive waveguides," *Appl. Phys. Lett.*, vol. 56, pp. 1409–1411, 1990.

[6] ——,"Single quantum-well laser with 11.2 degree transverse beam divergence," *Electron. Lett.*, vol. 26, pp. 1348–1350, 1990.

[7] S. T. Yen and C. P. Lee, "Theoretical investigation on semiconductor lasers with passive waveguides," *IEEE J. Quantum Electron.*, vol. 32, pp. 4–13, 1996.

[8] M. Ziari, J.-M. Verdiell, and D. F. Welch, "Low-loss coupling of 980 nm GaAs laser to cleaved single mode fiber," in *Proc. IEEE Lasers Electro-Opt. Soc. Annu. Meet., LEOS'95*, San Francisco, CA, Oct. 1995, pp. 5–6.

[9] D. Marcuse, "Solution of the vector wave equation for general dielectric waveguides by the Galerkin method," *IEEE J. Quantum Electron.*, vol. 28, pp. 459–465, 1992.

[10] J. Buus, "Beamwidth for asymmetric and multilayer semiconductor laser structures," *IEEE J. Quantum Electron.*, vol. 17, pp. 732–736, 1981.

[11] H. C. Casey, Jr., and M. B. Panish, *Heterostructure Lasers*, Part A. New York: Academic, 1978.

[12] D. C. Liu, C. P. Lee, C. M. Tsai, T. F. Lei, J. S. Tsang, W. H. Chiang, and Y. K. Tu, "Role of cladding layer thicknesses on strained-layer InGaAs/GaAs single and multiple quantum well lasers," *J. Appl. Phys.*, vol. 73, pp. 8027–8034, 1993.

[13] J. Temmyo and M. Sugo, "Design of high-power strained InGaAs/AlGaAs quantum-well lasers with a vertical divergence angle of 18°," *Electron. Lett.*, vol. 31, pp. 642–644, 1995.

Shun-Tung Yen, photograph and biography not available at the time of publication.

Chien-Ping Lee (M'80–SM'84), photograph and biography not available at the time of publication.